Journal of The Electrochemical Society, **153** (6) A1206-A1210 (2006)
0013-4651/2006/153(6)/A1206/5/$20.00 © The Electrochemical Society

In Situ Optical Observations of Particle Motion in Alloy Negative Electrodes for Li-Ion Batteries

A. Timmons* **and J. R. Dahn****,z**

Department of Physics and Atmospheric Science, Dalhousie University, Halifax, Nova Scotia B3H 3J5, Canada

Direct observation of the particles of active material as they react in situ is necessary to build an understanding of the interaction mechanisms present when large volume-change active materials are employed in composite electrodes. In situ optical observations of a-$Si_{0.64}Sn_{0.36}$ composite electrodes show dramatic interparticle movement; particles from below the electrode surface are pushed up, particles above the electrode surface shift downward, particles crash and overlap, particles become inactive, and some particles move so far that they become detached from the electrode.
 [DOI: 10.1149/1.2194611]

Manuscript submitted November 15, 2005; revised manuscript received December 27, 2005. Available electronically May 2, 2006.

Recently, much effort has been devoted to the search for negative electrode materials to replace carbon in lithium-ion batteries. The search has focused on metals and alloys that form alloys with lithium, offering up to a tenfold increase in specific and volumetric capacities.[1-24] Furthermore, research from a variety of groups including Sony, Graetz, and Dahn shows that amorphous alloys are preferable to crystalline alloys[25-27]; a-Sn, a-Ge, and a-Si-based alloys have displayed excellent capacity retention over many cycles.

Increased capacity necessitates increased volumetric expansion of a metal or alloy as it reacts with lithium. Reversible capacity necessitates reversible volumetric expansion. Patterned thin-film electrodes of an amorphous metallic alloy, fabricated *vis-à-vis* magnetron sputter deposition, can undergo reversible volume change, and exhibit excellent reversible capacity.[28,29] Composite electrodes containing particles of the same amorphous metallic alloy often exhibit some capacity fade.[30] Models and observations suggest that the particles of active material are not to blame for the capacity fade, but rather the electrode binder fails to accommodate the large volumetric expansions, resulting in electrically isolated particles and consequent capacity fade.[30] Without direct observations of particles as they react in situ, it is impossible to assert the validity of the assumption that large particle motion contributes to capacity fade.

Experimental

In order to directly observe the particles in a composite electrode as they react in situ, a microscope (mid-20th century Earnst Leitz Wetzlar) was machined such that it could be placed in an argon-filled glove box (Vacuum Atmospheres) and fitted with a digital camera (Logitech) to display and record the optical images on a computer (Fig. 1). All cell assemblies and electrochemical tests were performed in an argon-filled glove box.

The objective lens of the microscope had to see the surface of the electrode sample under study. To achieve this, an open Li-metal cell (wet cell) was employed (Fig. 2) that kept the Li metal reference and counter electrode out of the line of sight by moving it to the interior perimeter of a polypropylene well such that a 1 mL pool of transparent electrolyte could transfer the Li (as ions) to the sample electrode for in situ cycling. The electrolyte employed in the wet cell was a 1 M concentration of $LiPF_6$ salt dissolved in equal ratios of ethylene carbonate (EC) and propylene carbonate (PC). This electrolyte was chosen because of its very low volatility; in a glove box that was maintained at a temperature of 30°C and a gauge pressure of 49 Pa, the average evaporation rate was ~5 μL/day for a ~1 mL pool of electrolyte.

The electrode sample was illuminated by a fiber-optic lamp, which added negligibly to the temperature of the sample environment. The overall magnification of the microscope was 200× through the employment of a 10 times objective and a 20 times eyepiece. With the 200 times magnification optical microscope, it was possible to watch several particles interacting with each other and with the polymer binder in composite electrode samples.

Two composite electrodes, consisting of 71.4 wt % 10–20 μm particles of a-$Si_{0.64}Sn_{0.36}$ (3M Co.) in poly(vinylidene fluoride)-tetrafluoethylene-propylene (PVDF-TFE-P) (Dyneon Corp.) based binder were fabricated and observed in situ under different cycling conditions. The first sample was discharged to 0 V on every cycle, the second sample was discharged to 0.3, 0.2, 0.1, and 0.06 V for the first four respective cycles, and then to 0 V for every subsequent cycle. During each cycle the electrodes were charged to 1 V. The cycling was conducted at constant current (C/60, 8 μA for the first sample and 9.5 μA for the second sample) using a Keithley 236 source measure unit. The electrodes were fabricated according to the following procedure reported in Ref. 27: 10.038 g a-$Si_{0.64}Sn_{0.36}$, (3M Co.), 2.000 g Super-S carbon black (SS, MMM Carbon, Belgium), 5.028 g 20 wt % PVDF-TFE-P (Dyneon Corp.)

Figure 1. Optical microscope with an attached webcam modified for use in an argon-filled glove box.

* Electrochemical Society Student Member.
** Electrochemical Society Active Member.
z E-mail: jeff.dahn@dal.ca

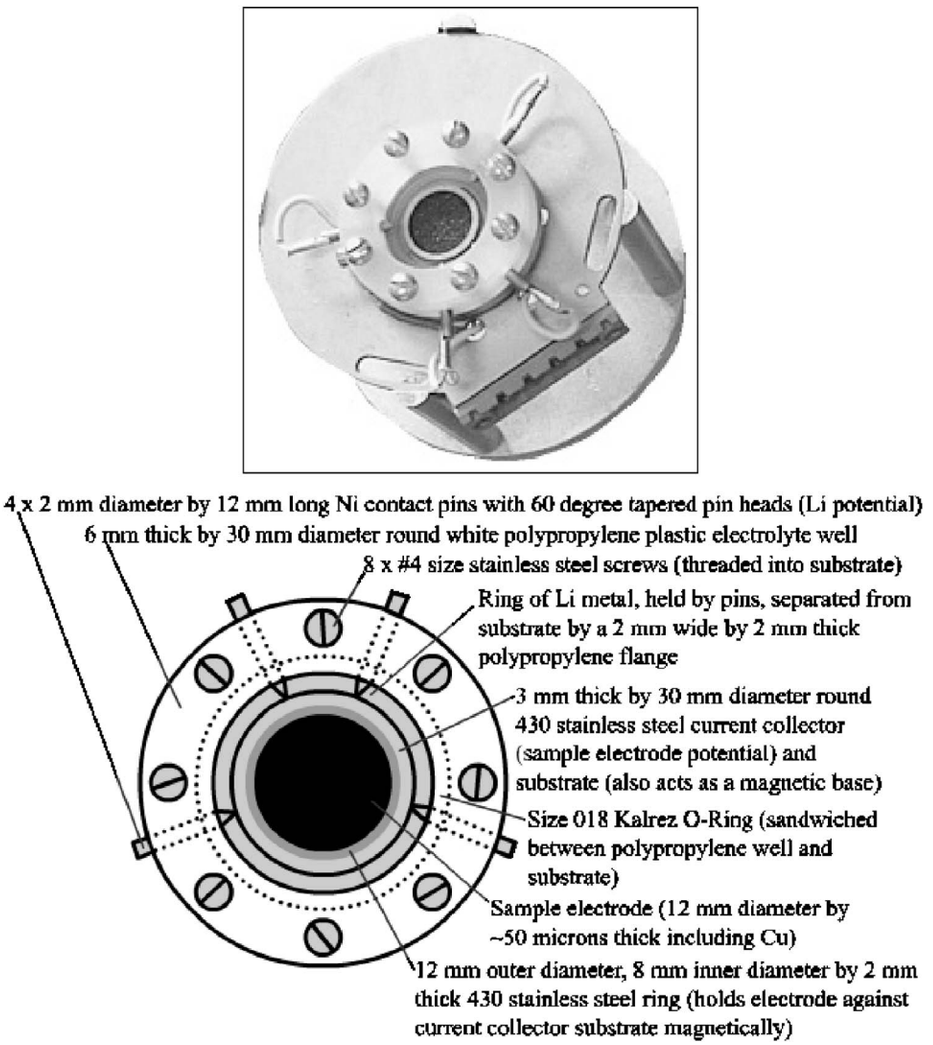

Figure 2. The "wet cell" stage holds the sample electrode in place such as to be viewed by a microscope as it cycles in situ vs lithium metal. Composite electrode samples (black disk) are held in place magnetically by a stainless-steel ring while immersed in an electrolyte contained in a polypropylene well. Nickel pins hold a ring of lithium metal to the inner perimeter of the polypropylene well when the wet cell is in use in a glove box.

solution in methyl ethyl ketone (MEK, Aldrich), 0.039 g CaO (Fisher Scientific), 0.031 g 1,4-diazabicyclo[2.2.2]octane (DABCO, Aldrich), and 0.477 g 3-aminopropyltriethoxysilane (AP, adhesion promoter, Aldrich) were added to a polypropylene bottle. The purpose of each of these additives is explained in Ref. 27 and 30. Then, 29.8 g MEK and about 10 zirconia milling media were added and the bottle was closed with its lid and shaken for 30 min to mix the slurry. After shaking, the slurry was spread as a bead along a straight line on a piece of flattened copper foil (10 μm thick) supported on a glass plate. Then, the slurry bead was spread in a perpendicular direction using a notch bar spreader with a gap between the bottom of the spreader and the top of the copper foil. The film was dried in air overnight and then cut into 1.27 cm^2 round electrodes before being heated in argon flow at 110°C for 24 h. The electrodes used for the optical observations had a dried deposition thickness of ~37 μm, corresponding to the region of column 8 with respect to the electrode array described in Ref. 27.

Results and Discussion

Figure 3 shows particles in the first sample undergoing dramatic movement within the electrode. Some particles of interest are enclosed either in a square, circle, or rectangle in each of the five images, which along with the electrode's potential curve compose the figure.

First, note the changing morphology of the two large particles contained in the superimposed square enclosure present in each image of Fig. 3. In image 1 the particles are well separated by a distance nearly equivalent to either particle's diameter. In image 2 the particles have grown and their separation has decreased substantially. In image 3 the particles have grown to such an extent that they have crashed into one another, forcing one particle to overlap the other, resulting in the dramatic upheaval of the left-hand particle with respect to the right-hand particle. Figure 4 shows quantitatively the physical distance separation between the initially closest points of the two large particles as a function of time correlated to the cell potential. The overlap seen in image 3 of Fig. 3 appears quantitatively as a negative physical separation. In image 4 the particles have decreased in size and are once again separated; however, their mutual separation has decreased, meaning that the particles have either taken in lithium that they are not able to liberate, or their position on the electrode has been permanently altered. Because the particles are composed of an active material that as a thin film has been shown to react reversibly with lithium over tens of cycles,[31] either reason for their new mutual separation distance must be an effect of the dramatic movement of the particles, as observed between images 1 and 3, causing irreparable local damage to the electrode binder. In image 5 the particles have once again grown and collided with one another; however, they have not reached the size they attained in image 3, indicating that they have not been able to store as much lithium. We suggest that this decrease in capacity is a

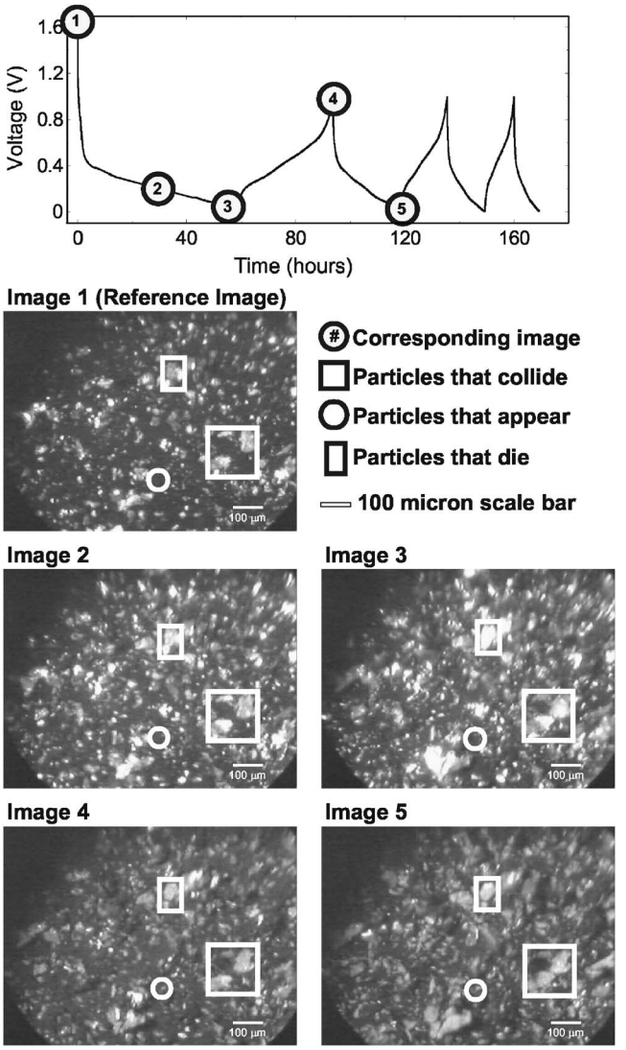

Figure 3. Voltage data (top) and images show the electrochemical and physical evolution of a ~37 μm thick composite electrode containing ~10–20 μm diameter particles of a-$Si_{0.64}Sn_{0.36}$ at 71.4% wt % in PVDF-TFE-P polymer binder containing 10 wt % super-S carbon as it cycles in situ at C/60 vs Li metal in ~1 mL of 1 M $LiPF_6$ in EC:PC electrolyte. Square enclosures: Notice that the particles grow together, crash into one another, overlap one another, shrink away from each other but are altered with respect to their relative starting positions on the electrode. Circular enclosures: Notice that initially there is an absence of any particles and by the final image particles are clearly observed. Rectangular enclosures: Notice that the size and shape of the upper particle remains unchanged between images 4 and 5 despite the charging of the electrode.

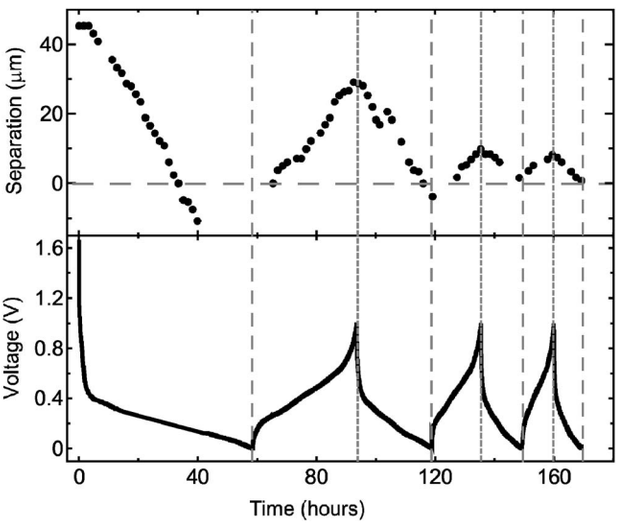

Figure 4. Plot showing the interparticle separation distance between the two particles contained in the square enclosures in Fig. 3. Notice that the particles move so much that they crash together and even overlap one another.

result of increased local electrical impedance caused by local damage to the electrode binder, which is a consequence of large volumetric changes in previous cycles.

Second, note the changing morphology of the electrode surface contained in the superimposed circular enclosure present in each image of Fig. 3. In image 1 the electrode surface appears featureless and therefore barren of any particles. In image 2 the electrode surface appears textured and there is a hint that a particle may be present just below the surface. In image 3 the texture has developed into a noticeable mound. In images 4 and 5 it is obvious that a small particle is contained in the enclosure. The emergence of a particle from below to above the surface of the electrode indicates that substantial particle movement is not limited to the surface of the electrode as seen by the microscope, but is also present within the electrode. We suggest that particles that undergo a large volume change will move, collide, and shuffle past one another as the electrode cycles. This kind of dramatic movement requires optimized binders that are designed to accommodate the movement while maintaining electrical contact between the particles in the electrode.

Third, note the changing morphology of the large particle contained in the superimposed rectangular enclosure present in each image of Fig. 3. In image 1 the particle is somewhat difficult to distinguish from its neighbors because it resides partially under the surface of the electrode. In image 2 the particle is easily distinguishable because it has grown and much of it resides above the electrode surface. In image 3 the particle has grown so substantially that it seems to have merged with its neighboring particles and together they nearly fill the entire rectangular enclosure. In image 4 the large particle is again easily distinguishable because its size has substantially decreased as a result of lithium removal. In image 5 the large particle has not changed size as compared to image 4. The lack of a noticeable change in dimension indicates that the particle has become electrically isolated to such a degree that it can no longer participate significantly in lithium storage. The particle has effectively spontaneously died! We suggest that the observation of the overall decrease in electrode capacity is not the result of an irreversible capacity loss inherent to the active material contained in the particles within the electrode, but is the result of local partial or complete electrical isolation of the particles from the electrode.

Figures 5 and 6, respectively, highlight the qualitative and quantitative behavior of two neighboring particles in the second sample that respond differently to a systematic reduction in lower cutoff potential. While dramatic interparticle movement was also observed in the second sample, that information has been cropped in order to magnify the behavior of the two neighboring particles enclosed in the superimposed circular enclosure present in each image of Fig. 5. The width of each image is one-quarter that of the images in Fig. 3. The neighboring particles are labeled top particle and bottom particles. In each image the top particle is enclosed in a thick-bordered rectangle, and the bottom particle is enclosed in a thin-bordered rectangle. The sizes of the thick and thin rectangles are such that the particles they contain just fit within the their inner perimeters; consequently, their sizes change from image to image commensurate with the changing sizes of the particles they contain.

The most significant feature present in Fig. 5, presented quantitatively in Fig. 6, is found through a comparison of particle sizes (areas as seen by the microscope) between images 6 and 7. On

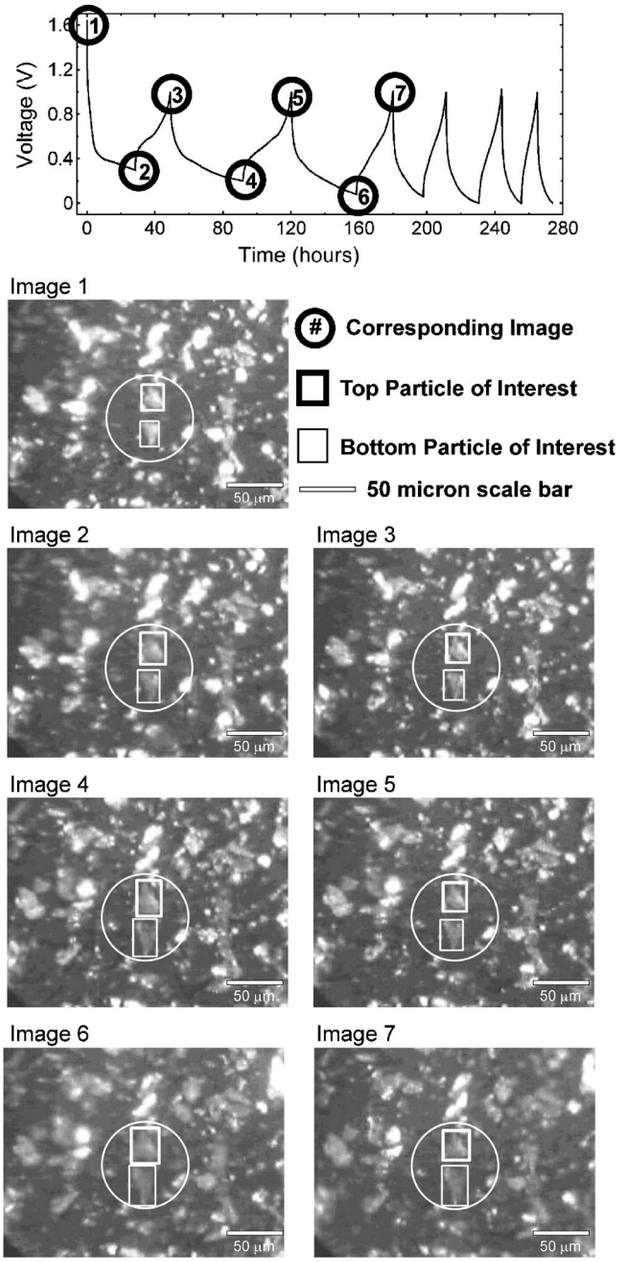

Figure 5. Voltage data (top) and images show the electrochemical and physical evolution of a ~37 μm thick composite electrode containing ~10–20 μm diameter particles of a-$Si_{0.64}Sn_{0.36}$ at 71.4% wt % in PVDF-TFE-P polymer binder containing 10 wt % super-S carbon as it cycles in situ at C/60 vs Li metal to 0.3, 0.2, 0.1, 0.06, and finally 0 V lower cutoff potentials in ~1 mL of 1 M $LiPF_6$ in EC:PC electrolyte. Images 1 through 7 highlight two neighboring particles that behave differently when subjected to a 0.2 V lower cutoff potential. Between images 5 and 6 both particles grow substantially as lithium is inserted up to the 0.1 V cutoff potential; however, between images 6 and 7 the top particle shrinks, whereas the bottom particle does not.

previous cycles both particles behaved similarly; they both grew larger as more lithium was incorporated during each discharge to lower cutoff potentials, and shrank as lithium was liberated during each charge to 1 V. Between images 6 and 7, as the electrode was charged from a lower cutoff potential of 0.1 to 1 V, the top particle behaved normally and shrank, whereas the bottom particle did not shrink. Figure 6 shows that, by the end of the discharge to 0.2 V, as

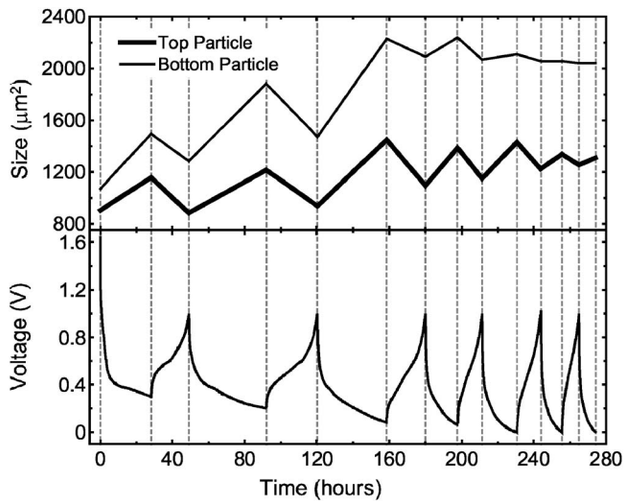

Figure 6. Plot showing the sizes of the two particles highlighted in Fig. 5 at the tops of charges and bottoms of discharges. The effect of discharging below a 0.2 V lower cutoff potential for this electrode is clearly demonstrated as first the bottom particle and eventually the top particle become electrically isolated and are no longer able to contribute to the capacity of the electrode.

compared to their initial sizes, the size of the top particle increased by about 50% and the size of the bottom particle increased by about 70%. By the end of the discharge to 0.1 V the size of the top particle increased by about 60% and the size of the bottom particle increased by about 100%. We suggest that, while the binder was able to accommodate (maintain low impedance electrical contact) the changes in sizes of the particles up to the end of the discharge to 0.2 V, it was not able to accommodate the change in size of the bottom particle at the end of the discharge to 0.1 V. This observation agrees with previous electrochemical testing on an identical electrode fabrication which showed that discharging to a lower cutoff potential of 0.2 V prolongs the cycle life of the electrode tremendously, whereas going to a 0.06 V lower cutoff potential supported many fewer cycles.[32] This suggestion is further supported by image 2 of Fig. 3. Image 2 corresponds to a cell potential of 0.2 V. While there is evidence of particle movement, the movement is much less severe at 0.2 V than at 0 V, as seen in image 3 of Fig. 3. We suggest that large volume change, high-capacity alloy negative active materials can be effectively employed in composite electrodes so long as their volume change is accommodated by either high-porosity, imposed lower cutoff potential, optimized binder, or most likely a combination thereof.

Both in situ experiments can be observed as time-lapsed animations by visiting http://fizz.phys.dal.ca/~dahn/movies2/

Conclusion

Large interparticle movement contributes to capacity fade through the electrical isolation of particles in composite electrodes containing particles composed of large volume change active materials. We suggest that improved cycling performance by limiting the lower cutoff potential (lithium content) is due to decreased interparticle movement that increases with lithium content. In order to use particles composed of large volume change active materials in a composite electrode, cycling procedures and binder systems that are capable of accommodating the large interparticle movements have to be employed.

Acknowledgments

The authors acknowledge the support of this research by the Natural Sciences and Engineering Research Council (NSERC) of Canada. A.T. acknowledges NSERC and Dalhousie University for financial support.

Dalhousie University assisted in meeting the publication costs of this article.

References

1. M. Winter and J. O. Besenhard, *Electrochim. Acta*, **45**, 31 (1999).
2. Y. Idota, A. Matsufuji, Y. Maekawa, and T. Miyasaki, *Science*, **276**, 1395 (1997).
3. O. Mao, R. L. Turner, I. A. Courtney, B. D. Fredericksen, M. I. Buckett, L. J. Krause, and J. R. Dahn, *Electrochem. Solid-State Lett.*, **2**, 3 (1999).
4. C. J. Wen and R. A. Huggins, *J. Electrochem. Soc.*, **128**, 1636 (1981).
5. J. Wang, I. D. Raistrick, and R. A. Huggins, *J. Electrochem. Soc.*, **133**, 457 (1986).
6. J. Yang, M. Wachtler, M. Winter, and J. O. Besenhard, *Electrochem. Solid-State Lett.*, **2**, 161 (1999).
7. I. A. Courtney, J. S. Tse, O. Mao, J. Hafner, and J. R. Dahn, *Phys. Rev. B*, **58**, 15583 (1998).
8. R. A. Huggins, in *Handbook of Battery Materials*, J. O. Besenhard, Editor, Part III, Chap. 5, Wiley-VCH, Weinheim (1999).
9. P. Poizot, S. Laurelle, S. Grugeon, L. DuPont, and J.-M. Tarascon, *Nature (London)*, **407**, 496 (2000).
10. J.-M. Tarascon and M. Armand, *Nature (London)*, **414**, 359 (2001).
11. M. Egashira, H. Takatsuji, S. Okada, and J. Yamaki, *J. Power Sources*, **107**, 56 (2002).
12. Y. Xia, T. Sakai, T. Fujieda, M. Wada, and H. Yoshinaga, *J. Electrochem. Soc.*, **148**, A471 (2001).
13. A. Netz and R. Muggins, *J. Power Sources*, **119**, 95 (2003).
14. X. B. Zhao and G. S. Cao, *Electrochim. Acta*, **46**, 891 (2001).
15. G. A. Roberts, E. J. Cairns, and J. A. Reimer, *J. Power Sources*, **110**, 424 (2002).
16. J. O. Besenhard and M. Winter, *Phys. Chem. Chem. Phys.*, **3**, 155 (2002).
17. R. Alcantara, M. Jaraba, P. Lavela, and J. L. Tirado, *J. Solid State Chem.*, **166**, 330 (2002).
18. M. Yoshio, H. Wang, K. Fukuda, T. Umeno, N. Dimov, and Z. Ogumi, *J. Electrochem. Soc.*, **149**, A1598 (2002).
19. H. Li, X. Huang, L. Chen, G. Zhou, Z. Zhang, D. Yu, Y. J. Mo, and N. Pei, *Solid State Ionics*, **135**, 181 (2000).
20. J. H. Ryu, J. W. Kim, Y. E. Sung, and S. M. Oh, *Electrochem. Solid-State Lett.*, **7**, A306 (2004).
21. Y. S. Fung and D. R. Zhu, *J. Electrochem. Soc.*, **149**, A319 (2002).
22. I. Sandu, T. Brousse, D. M. Schleich, and M. Danot, *J. Solid State Chem.*, **177**, 4332 (2004).
23. H. Jung, M. Park, S. H. Han, H. Lim, and S. K. Joo, *Solid State Commun.*, **125**, 387 (2003).
24. S. Laruelle, P. Poizot, E. Baudrin, V. Briois, M. Touboul, and J.-M. Tarascon, *J. Power Sources*, **97**, 251 (2001).
25. Japan Sony Corp., *Sony Press Release* 05-006E, Tokyo (Feb 15 2005).
26. J. Graetz, C. C. Ahn, R. Yazami, and B. Fultz, *J. Electrochem. Soc.*, **151**, A698 (2004).
27. Z. Chen, V. Chevrier, L. Christensen, and J. R. Dahn, *Electrochem. Solid-State Lett.*, **7**, A310 (2004).
28. L. Y. Beaulieu, K. W. Eberman, L. J. Krause, and J. R. Dahn, *Electrochem. Solid-State Lett.*, **4**, A137 (2001).
29. L. Y. Beaulieu, T. D. Hatchard, A. Bonakdarpour, M. D. Fleischauer, and J. R. Dahn, *J. Electrochem. Soc.*, **150**, A1457 (2003).
30. Z. Chen, L. Christensen, and J. R. Dahn, *Electrochem. Commun.*, **5**, 919 (2003).
31. T. D. Hatchard and J. R. Dahn, *J. Electrochem. Soc.*, **151**, A1628 (2004).
32. Z. Chen, L. Christensen, and J. R. Dahn, *J. Appl. Polym. Sci.*, **91**, 2949 (2004).